



OPEN Study on prediction method of parameters behind target of jet under dynamic conditions

Xuepeng Zhang¹, Can Xu², Yizhen Wang¹, Jianping Yin¹✉, Jianya Yi¹ & Xudong Li¹

To systematically characterize the post-target behavior of shaped charge jets under dynamic conditions, this study establishes a finite element model for jet penetration through finite-thickness moving targets, elucidating the evolutionary dynamics of jet interaction under lateral disturbances. By integrating virtual origin theory and dimensional analysis, a virtual source parameter is introduced to quantify post-target jet metrics. An engineering predictive model is further developed to describe the residual velocity and post-target diameter of jets under lateral perturbations. Static and dynamic penetration experiments validate the numerical simulations and theoretical framework. Results reveal that residual jet velocity decays exponentially with increasing lateral disturbance, while post-target diameter exhibits exponential growth. Strong agreement among numerical predictions, model outputs, and experimental data confirms the accuracy of the proposed framework. This work provides a validated methodology for assessing the post-target performance of shaped charges in dynamic scenarios.

Keywords Shaped charge jet, Impact, Lateral disturbance, Dimensional analysis, Dynamic test

Shaped charge jets (SCJs) technology plays an increasingly important role in the field of hypervelocity impact and fluid mechanics, especially in the study of the interaction between high-speed fluid and materials, impact response and dynamic behavior of engineering structures. During the penetration process, complex fluid dynamics and shock wave propagation phenomena occur between the jet and the target. The velocity of the jet, the response of the target plate, the interaction between the fluid and the solid interface and other factors jointly determine the behavior and effect of the hypervelocity impact. Therefore, it is of great significance to study the dynamic behavior of SCJ, especially the response process under the condition of high-speed impact, for improving the engineering structure and optimizing the related application technology. The hypervelocity impact behavior of SCJ includes the formation and propagation of jet and the dynamic response of target plate. The study of this process needs to consider many factors such as fluid dynamics, impact mechanics and material mechanics.

Since the SCJ is a fluid-like medium, it is quite different from the common solid material characteristics. Therefore, it has certain research significance for investigating its mechanical and engineering characteristics after lateral disturbance. Under dynamic conditions, the jet will be affected by significant lateral disturbance during the penetration process, which is quite different from the common static penetration process. Specifically, the jet may deflect, destabilize and fracture during penetration. Therefore, in order to obtain the jet characteristics and mechanical response of the SCJ after penetrated the finite thickness plate under the condition of dynamic intersection, it is necessary to seek a parameter to characterize it, and establish a prediction model to estimate and analyze its variation law.

For the study of the penetration performance of shaped charge jet, many scholars have made many achievements¹⁻⁵. For the dynamic penetration process of jet under lateral disturbance, domestic and foreign scholars have also carried out some research. Helte⁶ analyzed the cause of the disturbance caused by the interaction between the jet and the flying plate of the reactive armor; Frankel et al.⁷ analyzed the influence of target lateral motion on projectile penetration performance by using fluid dynamics model, and studied the change of penetration velocity and streamline shape with the corresponding ratio of target to projectile velocity and density. Cao Peng et al.⁸ analyzed the penetration process of three different shaped charge damage elements into high-speed moving target plates; Luttwak et al.⁹ established a yaw model and studied the erosion of the long rod during the perforation of the moving plate and the possible bending or deflection of the residual rod through numerical simulation. Li et al.¹⁰ designed a compressible model of shaped charge jet penetrating radial reaming;

¹School of Mechanical and Electrical Engineering, North University of China, Taiyuan 030051, Shanxi, China. ²Anhui Dongfeng Mechanical and Electrical Technology Co., Ltd., Hefei 23002, Anhui, China. ✉email: yjp123@nuc.edu.cn

Yadav¹¹ studied the interaction between shaped charge jet and moving target on the basis of simplifying the assumption of constant velocity of jet and target. Han¹² numerically simulated the penetration process of the shaped charge jet into the moving target plate under different incident angles, and obtained the basic laws of the penetration ability of the shaped charge jet in oblique penetration. Zhu Dingbo et al.¹³ used experiments to analyze the changes of explosive armor interference during jet penetration.

According to the published literature, most scholars' research on the penetration behavior response of SCJ mainly focuses on the further expansion of the static penetration power of SCJ or the analysis of the jet disturbance of thin-walled targets^{2,14,15}. At present, the engineering prediction models of the residual velocity and diameter of the laterally disturbed jet penetrating the finite thick target are rarely published, and most of them are the research on the critical initiation threshold K of the jet on the shielded explosive under dynamic conditions; However, there is little research on the behavior characteristics and characterization methods of the jet after penetrating the finite thick target under dynamic conditions, especially the dynamic penetration test of SCJ jet under high-speed lateral disturbance and the prediction model of the characteristic parameters behind the target under dynamic conditions. Therefore, this paper focuses on the characterization and engineering prediction of the performance parameters of the jet passing through a finite thickness target under dynamic conditions. The dynamic penetration process of jet under lateral disturbance is numerically simulated, and the dynamic penetration process of jet is analyzed. Then, based on the virtual origin and dimensional analysis method, the virtual source position is taken as the characterization of the jet, which solves the problem that it is difficult to effectively characterize SCJ based on a single structural parameter in the dimensional analysis model. The prediction model of the characteristic parameters behind the jet target under dynamic conditions is established. Finally, the jet dynamic penetration test under the condition of high-speed missile target rendezvous was carried out on the rocket sled as the experimental platform, and the validity and applicability of the prediction model were verified by the experimental data.

Model and research plan

Simplified model and numerical simulation

The shaped charge structure consists of a shell, a mounting ring, a main-charge, a sub-charge, a wave shaper and a liner. The bottom center initiation method is adopted. The simplified model of shaped charge is shown in Fig. 1. The shell is aluminum alloy, the liner is copper, the charge is comp B explosive, and the waveform regulator is phenolic resin. The liner diameter is 90 mm and the charge length is 180 mm. The liner is a cone with equal wall thickness, the wall thickness is 1.55 mm, and the cone angle of the liner is 45°. Considering the symmetry of the dynamic penetration process of the SCJ, the numerical simulation adopts a half model of 1:1 size.

The target plate adopts the Lagrangian algorithm, and the remaining components adopt the Euler algorithm. The model uses the fluid-solid coupling algorithm to simulate the forming process of the jet and its penetration process into the target plate. The Euler algorithm can better simulate the forming and penetration process of the shaped jet. The large deformation process caused by dynamic conditions. The model element meshes are all hexahedral elements. Numerical calculations are conducted in the air domain. The traditional ALE algorithm requires a large amount of spatial grid and consumes a lot of time. Although the structured arbitrary Lagrangian Euler (S-ALE) algorithm has the same computational process as traditional ALE algorithms, the S-ALE algorithm has advantages such as simple grid generation, high computational efficiency, and strong computing power. Therefore, this article uses the S-ALE algorithm to generate air grids. Automatically fill wave shaper, explosives and liner. The numerical simulation model adopts the g-cm- μ s element system.

In order to simulate the propagation process of explosive in the real-world scene, combined with the formation process of SCJ and the pressing mechanism of detonation wave on the liner, the air domain is maintained in the area where the charge acts on the liner, and the non-reflective boundary is set on the surface of the air outside the finite element model, so that the explosive flows out freely. It is used to reduce the calculation time of numerical simulation while maintaining the accuracy of calculation. Figure 2 is the numerical simulation model of jet dynamic penetration. The grid size of the air domain is 1 mm \times 1 mm \times 1.5 mm, the thickness of the target plate is 100 mm, and the grid size of the target plate is 1 mm \times 1 mm \times 1 mm. In order to avoid the boundary effect affecting the accuracy of the numerical simulation results, the position where the jet will not contact directly outside the target plate is set by setting the transition grid method to increase the size of the target plate and improve the operation efficiency.

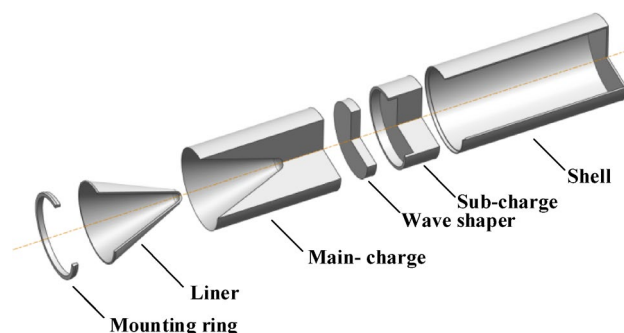


Fig. 1. Simplified model of shaped charge.

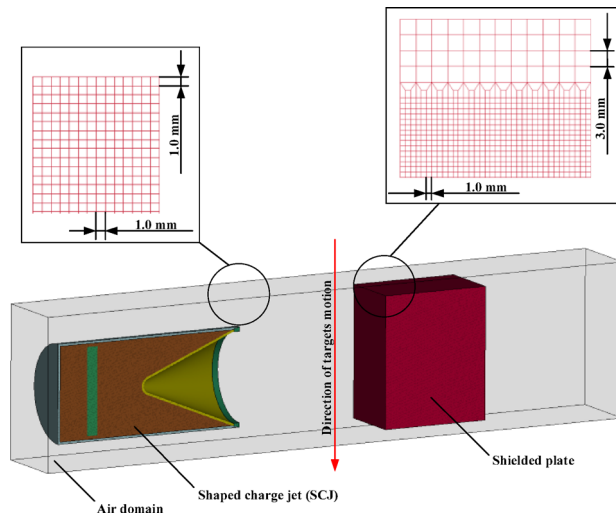


Fig. 2. Numerical simulation model of jet dynamic penetration.

Material	$\rho/\text{kg}\cdot\text{m}^{-3}$	A/GPa	B/GPa	C	M
Copper	8960	0.09	0.290	0.025	1.09

Table 1. Material parameters of liner.

Parameters	Values	Parameters	Values
$\delta/(\text{kg}\cdot\text{m}^{-3})$	1717	R_1	4.2
$D/(\text{m}\cdot\text{s}^{-1})$	8320	R_2	1.1
P_{CJ}	0.37	E_0	0.102
A/GPa	524.23	ω	0.34
B/GPa	7.68		

Table 2. Material parameters of explosive.

Material and parameters

Johnson–Cook material model and GRUNEISEN equation of state¹⁶ are used to describe the strength properties of materials that can withstand large strain and high strain rate. The parameters are shown in Table 1.

Among them, A is the initial yield stress of the material at the reference strain rate gas and the reference temperature, B and N are the strain hardening modulus and hardening index of the material at the reference strain rate and the reference temperature, respectively, C is the material strain rate strengthening parameter, and M is the material thermal softening parameter.

The charge adopts HIGH EXPLOSIVE BURN material model, and the state equation is JWL¹⁷. The material parameters and equation of state are derived from Reference¹⁸:

$$P = A \left(1 - \frac{\omega}{R_1 V}\right) e^{-R_1 V} + B \left(1 - \frac{\omega}{R_2 V}\right) e^{-R_2 V} + \frac{\omega E_0}{V'} \tag{1}$$

where P is the isentropic pressure; v is the relative volume of detonation products; E_0 is the initial internal energy. A , B , R_1 , R_2 and ω are constants, which are measured by the cylinder test of explosives. P_{CJ} is CJ pressure, and the relevant parameters are shown in Table 2.

The material of the shell and the retaining ring is aluminum alloy, and the explosive and the liner are tightly fixed together by using the retaining ring. The target material is 30CrMnMoRE. The material of waveform regulator is phenolic resin. The PK constitutive model is selected to describe the shell, mounting ring, wave shaper and target¹⁹. The material parameters of shell, waveform regulator and target plate are shown in Table 3.

Among them, E is Young’s modulus, ν is Poisson’s ratio, and σ_Y is the yield stress of the material.

Materials	$\rho/\text{kg}\cdot\text{m}^{-3}$	E/GPa	ν	σ_y/GPa	β
2024-T3 Aluminum alloy	2780	72.4	0.33	0.345	0.5
Phenol formaldehyde resin	1130	0.35	0.36	0.12	1
30CrMnMoRE	7830	202.8	0.3	0.975	1

Table 3. Material parameters of shell, wave shaper and target plate.

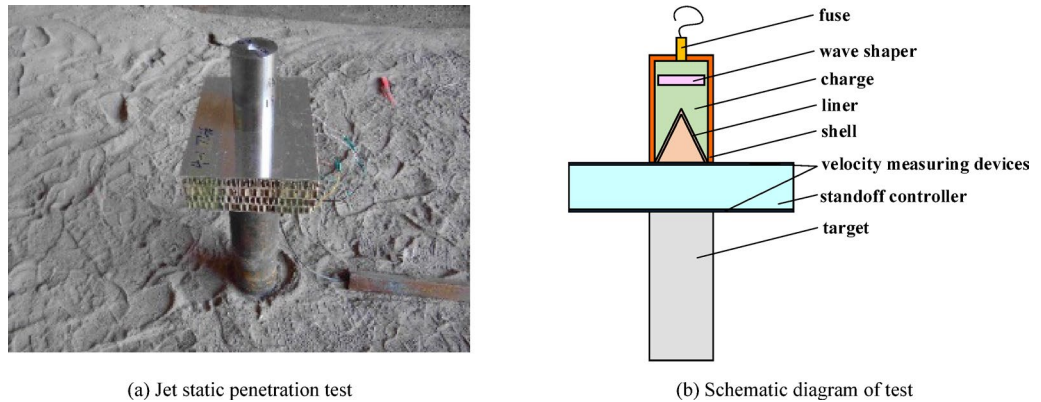


Fig. 3. SCJ static penetration test. (a) Jet static penetration test, (b) Schematic diagram of test.

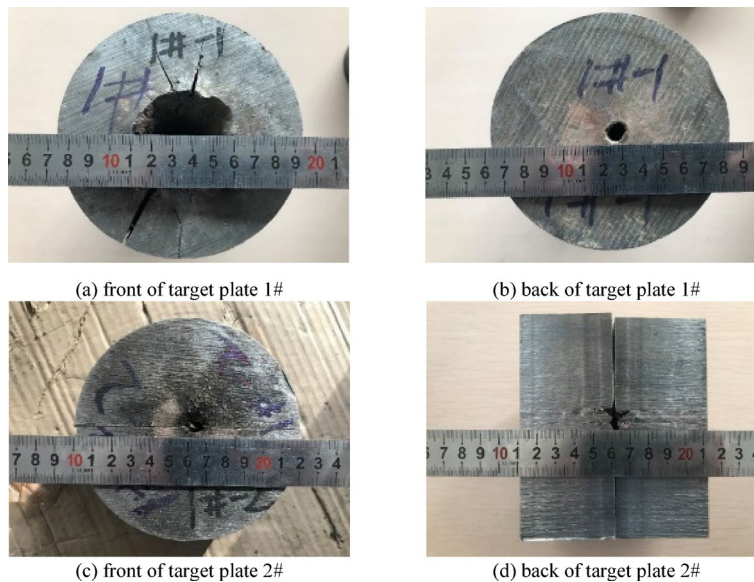


Fig. 4. Results of SCJ static penetration test. (a) front of target plate 1#, (b) back of target plate 1#, (c) front of target plate 2#, (d) back of target plate 2#.

Validation of numerical simulation

Considering the problem of large data distribution in dynamic test, in order to verify the accuracy of numerical simulation results and minimize the influence of data walk on the effectiveness of numerical simulation, the static test of shaped charge jet is used to investigate the effectiveness of numerical simulation.

For the static penetration power test of jet, in order to make the test results reliable with numerical simulation, the shaped charge structure and materials, numerical simulation model and finite element parameters used in the actual experiment are the same as those given in Sect. "Simplified model and numerical simulation" and "Material and parameters", only keeping the target plate in a static state.

The structure of the shaped charge used in the test is the same as that in the numerical simulation. Figure 3a is the test layout of the jet static test, and the test principle is shown in Fig. 3b.

It can be seen from Fig. 4 that the jet penetrates the first layer of the target plate, leaving some small holes on the second layer of the target plate, and the jet penetrates a total of about 305 mm of the target plate.

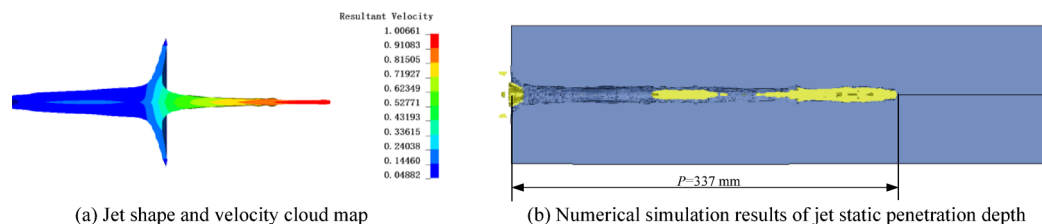


Fig. 5. Numerical simulation of SCJ static penetration. **(a)** Jet shape and velocity cloud map, **(b)** Numerical simulation results of jet static penetration depth.

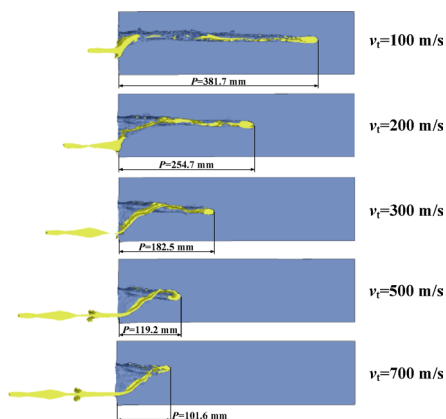


Fig. 6. The morph of SCJs penetrated the moving infinite plate.

In this regard, in the numerical simulation, the static penetration process of the jet under the same working conditions is numerically simulated, and the head velocity when the jet hits the target and the static penetration depth of the target plate are obtained, as shown in Fig. 5.

The head velocity of the jet in numerical simulation is $10006.1 \text{ m}\cdot\text{s}^{-1}$, and the experimental data is $9666.67 \text{ m}\cdot\text{s}^{-1}$. The relative error between the two is 3.51%. The numerical simulation result of jet static impact through a semi-infinite target plate is 337 mm, and the relative error between the numerical simulation result and the experimental result is about 10.49%. This is mainly because in actual testing, the target plate is stacked with two layers of target plates, which causes a certain amount of energy loss during the impact process of the jet. When the jet contacts the second layer of target plate, it needs to start digging again and complete the impact. At this time, the head velocity of the jet has already caused significant loss when penetrating the first layer of target plate, thus affecting the impact process of the formed jet.

In addition, considering that in actual experiments, the energy gathering charge is also affected by factors such as processing technology and processing errors of various components, further increasing the difference between experiments and numerical simulations. Due to the ideal neglect of various influencing factors in numerical simulations, the numerical simulation results are slightly larger than the actual experiments.

However, combining the results of numerical simulation and static experiments, it can be seen that numerical simulation can still accurately simulate the actual jet impact process. Therefore, the next step is to use numerical simulation to reliably characterize the dynamic impact process of the jet.

Typical process of jet dynamic impact

In analyzing the typical dynamic penetration process of shaped charge jet, firstly, the process of jet penetration into semi-infinite target under different transverse disturbance velocity is numerically simulated to study and analyze the jet penetration depth under different transverse disturbance velocity. When the transverse disturbance velocity is 100–700 m/s, the penetration process and penetration depth of the shaped charge jet to the moving target are shown in Fig. 6.

The dynamic impact results of shaped charge jet with transverse disturbance velocity $v_t = 100\text{--}700 \text{ m/s}$ are shown in Fig. 6. When $v_t = 100 \text{ m/s}$, the disturbance effect of the transverse motion of the target plate on the jet impact initially appears. Due to the transverse action of the target plate, it cannot flow normally along the normal direction of the jet channel, but collides with the surface of the target plate and flows into the channel after deformation and offset. A large opening is left on the target entry surface. The jet which has the ability of breaking armor and has not completed the impact in the impact channel bends and breaks, and interacts with the hole walls on both sides, so that the depth of breaking armor is reduced. With the increase of the transverse disturbance velocity, the disturbance of the target motion on the jet impact continues to increase. The incompletely consumed jet in the impact channel deviates from the normal due to the transverse velocity, and

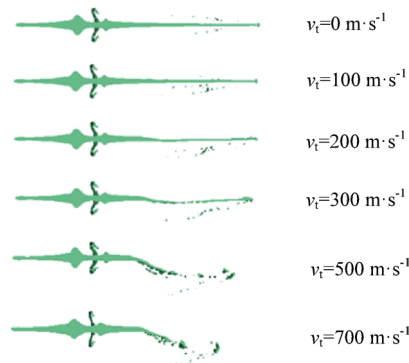


Fig. 7. The morph of SCJs penetrated the dynamic finite thickness plate.

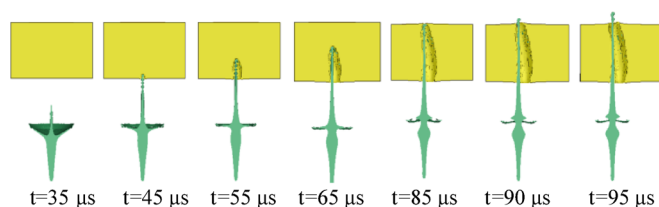


Fig. 8. SCJ-target interaction process under dynamic conditions.

then bends and breaks. The broken jet fragments interact with the hole wall twice, and the jet with the ability to impact appears obvious fracture and drift in the process of dynamic impact.

Further, considering that this study mainly focuses on finite thickness plates, in order to study the effect of shaped charge jet on finite thickness targets under different dynamic conditions, the relative velocity of shaped charge jet on 100 mm thick targets in the range of 0–750 m/s is given in the numerical simulation. The shape of the jet penetrating the target plate is shown in Fig. 7.

From Fig. 7, it can be seen that with the increase of relative velocity, the jet gradually bends and breaks after penetrating the target plate. The greater the relative velocity, the more serious the bending and fracture of the jet. The reason is that the movement of the target plate will exert a transverse force perpendicular to the axis on the jet. With the increase of the moving speed of the target plate, the transverse interference of the target plate on the jet will become stronger and stronger, which will eventually lead to the bending and fracture of the jet.

In order to further analyze the interaction between the target and the jet under dynamic conditions, the jet-target interaction at $v_i = 100$ m/s is selected for analysis, as shown in Fig. 8.

Under the action of detonation products, the shaped charge liner converges to the axis to form a shaped charge jet. At 40 μ s, the shaped charge jet is basically formed. At this time, the head velocity of the jet is 7169 $\text{m}\cdot\text{s}^{-1}$. At 45 μ s, the shaped charge jet contacts the target plate and penetrates the target plate. At 45–65 μ s, the jet opens a pit on the target plate. Because the jet can be regarded as a dense and viscous fluid-like medium, while the jet penetrates the target plate, the jet part that loses most of the energy and cannot carry out subsequent penetration expands around under the impetus of the subsequent jet, squeezing and expanding the hole wall. At the same time, it is affected by the lateral movement of the target plate. The jet begins to expand horizontally to form an inclined channel. At 95 μ s, the jet penetrates the target plate, and the velocity of the jet head decays to 4038 $\text{m}\cdot\text{s}^{-1}$.

Establishment of prediction model

Prediction model of jet residual velocity

Dimensional analysis is an effective tool to solve contemporary engineering problems, and it has a wide range of applications. Usually, although the same physical quantity can be expressed in different units, its dimension is fixed. Physical quantities have dimensional properties, so it is necessary to ensure that the dimensions on both sides of the equation are consistent when using mathematical formulas to describe the potential laws of the corresponding problems. This principle is called the principle of dimensional consistency. Based on the principle of dimensional consistency, the analysis of the relationship between physical quantities in the research problem is dimensional analysis.

For the problem of dynamic penetration behavior response of shaped charge jet, the dimensional analysis of the physical quantities affecting the results is carried out. For the analysis of the research situation in this paper, the charge composition is the same under different working conditions. Therefore, the factors such as charge density, charge detonation velocity and charge energy density can be ignored. Due to the complexity of the dynamic penetration process of the jet, the density and strength of the jet and the target material play an important role, so it cannot be ignored.

The shaped charge jet forming and the penetration process under lateral disturbance are investigated. It is found that many parameters of the shaped charge warhead, such as the cone angle, wall thickness, caliber and explosion height of the liner, are strongly coupled with each other, and the influence on the penetration depth of the jet is interrelated and very complicated. Therefore, in the process of establishing a dimensional analysis model, it is not possible to simply separate one of the single factors.

Since the research on the dynamic penetration power of shaped charge jet is mainly aimed at the structure of single cone shaped charge liner, the theory of quasi-steady penetration based on shaped charge jet is considered, and the hypothesis of virtual source is introduced. The position of virtual source is used to characterize the jet. The ideal assumption in the quasi-steady theory is that the velocity of each element on the virtual source is linearly distributed. Based on the quasi-steady penetration theory considering the strength of target and jet, there is:

$$P(t) = f(v_{j0}, t_0, v_{jc}, \gamma, v_j, S) \quad (2)$$

Among them, v_{j0} is the jet target velocity; t_0 is the time when the virtual source moves to the target plate; v_{jc} is the critical penetration velocity of the jet; v_j is the jet micro-element velocity at the interface of the jet and plate; $\gamma = \sqrt{\frac{\rho_t}{\rho_j}}$, where, ρ_t and ρ_j are the density of target plate and jet; S is the distance from the virtual source to the target surface.

Because of $S = v_{j0}t_0$, formula (2) can be rewritten as follows:

$$P(t) = f(v_{j0}, v_{jc}, v_j, t_0, \rho_j, \rho_t) \quad (3)$$

It can be known from the quasi-steady theory $V_{jc} = \sqrt{\frac{2\sigma}{\lambda\rho_j}}$, $\sigma = \sigma_t - \sigma_j$, there is:

$$P_{mj} = f(v_{j0}, v_j, t_0, \rho_j, \rho_t, \sigma_t, \sigma_j, \lambda) \quad (4)$$

In this equation, λ is a constant, $\lambda = 1$ for continuous jet.

For the case studied in this paper, the standoff of SCJ is about 1.5 times the liner diameter (1.5D). Compared with the traditional static shaped charge jet, the optimal burst height (3-4d) is significantly smaller, so in this case, the jet can effectively maintain continuity in the process of forming and penetration, so the ideal assumption is continuous penetration behavior. Since the jet standoff height in this study is small, the dynamic penetration process of the jet is regarded as continuous penetration, so λ takes 1.

At this time, the influence of the transverse velocity v_t of the target plate is added to investigate the residual head velocity $v_{j,dyn}$ after the jet penetrates the finite thickness target plate, which is:

$$v_{j,dyn} = f(T, v_{j0}, t_0, \rho_j, \rho_t, \sigma_t, \sigma_j, \lambda, v_t) \quad (5)$$

where T is the thickness of the target plate with finite thickness.

The jet impact velocity v_{j0} , the time t_0 of the jet micro-element moving from the virtual source to the target plate and the target plate density ρ_j are selected as the reference physical quantities. The dimensional index is recorded as matrix X , and the determinant of the dimensional index matrix is:

$$|X| = \begin{vmatrix} 0 & 0 & 1 \\ 1 & 0 & -3 \\ -1 & 1 & 0 \end{vmatrix} = 1 \neq 0 \quad (6)$$

It can be seen from Eq. (6) that the determinant is not zero and the dimensions of the three reference quantities are independent, indicating that any one of the reference quantities cannot be represented by the other two reference quantities, so the three reference quantities can be used as a set of basic quantities. The dimension index of the physical quantity is expressed as a vector y_i , then y_i can be obtained by linear transformation of the vector in the matrix X . This means that the remaining physical quantities can be obtained by linear transformation of the reference physical quantities. Through the dimensionless analysis of $v_{j,dyn}$, the form of dimensionless function relation can be obtained:

$$\frac{v_{j,dyn}}{v_{j0}} = f\left(\frac{T}{v_{j0}t_0}, \frac{\rho_t}{\rho_j}, \frac{\sigma_t}{v_{j0}^2\rho_j}, \frac{\sigma_j}{v_{j0}^2\rho_t}, \frac{v_t}{v_{j0}}\right) \quad (7)$$

In order to analyze the influence of each variable on the dynamic penetration power of the jet, the relationship between the dimensionless variables $v_{j,dyn}/v_{j0}$ and v_t obtained by numerical simulation is drawn in Fig. 9.

It is found that there is a good exponential relationship between $v_{j,dyn}/v_{j0}$ and various factors, so the respective variables are coupled in an exponential form; combined with the Π theorem, the term of the transverse velocity of the target plate is constructed. When the transverse velocity of the target plate $v_t=0$, the π_5 term degenerates into a constant term. At this time, $v_{j,dyn}$ are independent of v_t , $v_{j,dyn}$ degenerate into v_j . Then Eq. (7) is transformed into the following:

$$\frac{v_{j,dyn}}{v_{j0}} = R\left(\frac{T}{v_{j0}t_0}\right)^a \left(\frac{\rho_t}{\rho_j}\right)^b \left(\frac{\sigma_t}{v_{j0}^2\rho_j}\right)^c \left(\frac{\sigma_j}{v_{j0}^2\rho_t}\right)^d \left(A^{\xi} \frac{v_t}{v_{j0}}\right)^e + \chi \quad (8)$$

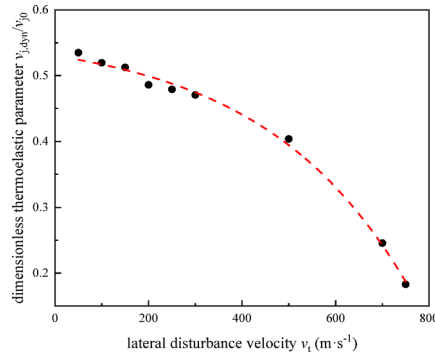


Fig. 9. The relationship between $v_{j,dyn}/v_{j0}$ and v_t .

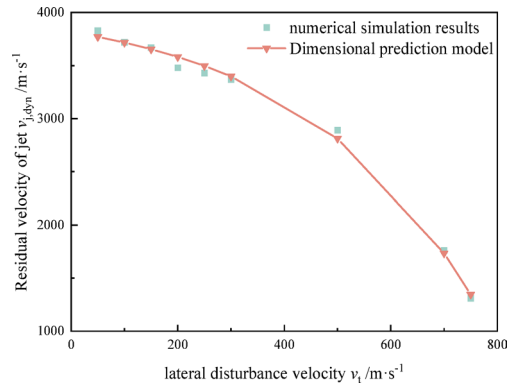


Fig. 10. v_t - $v_{j,dyn}$ dimensional prediction curve.

Among them, R, A, a, b, c, d and e are undetermined coefficients.

Since this paper focuses on the influence of the transverse velocity v_t of the target plate on the dynamic residual head parameter $v^2 d_{dyn}$, v_{j0} , t_0 , ρ_j , ρ_t , σ_j , σ_t , T remain unchanged under different working conditions, these physical quantities can be ignored in the dimensional analysis of this paper. Formula (8) is simplified to :

$$\frac{v_{j,dyn}}{v_{j0}} = R \left(A \xi \frac{v_t}{v_{j0}} \right)^e + \chi \tag{9}$$

In order to determine the value of the undetermined coefficient in the above expression, the simulation data results are statistically analyzed. Based on the numerical simulation results, the fitted functional relationship is obtained :

$$\frac{v_{j,dyn}}{v_{j0}} = -0.039 \left(3.423^{13.322} \frac{v_t}{v_{j0}} \right)^{1.332} + 0.572 \tag{10}$$

It can be seen from Fig. 10 that the results of dimensional analysis and numerical simulation are highly consistent, and the relative error of each group of data is below 10%.

Prediction model of jet diameter behind target

Similar to the prediction model of the residual velocity of the jet, combined with the functional relationship between the jet aperture and the penetration depth given in Reference⁵, the dimensional analysis of the diameter d_{dyn} behind the jet target is carried out, and the relationship between the dimensionless variable d/T and v_t is drawn in Fig. 11.

It is found that there is a good exponential relationship between d/T and various factors, so the respective variables are coupled in an exponential form; combined with the principle of dimensional analysis, the following is obtained:

$$\frac{d_{dyn}}{T} = R \left(\frac{v_t t_r}{T} \right)^a \left(\frac{v_{j,dyn} t_r}{T} \right)^b + \chi \tag{11}$$

Based on the numerical simulation results, the fitted functional relationship is obtained:

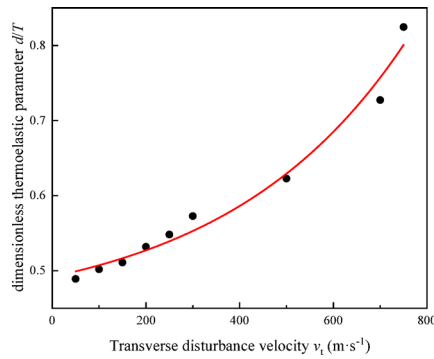


Fig. 11. The relationship between d/T and v_t .

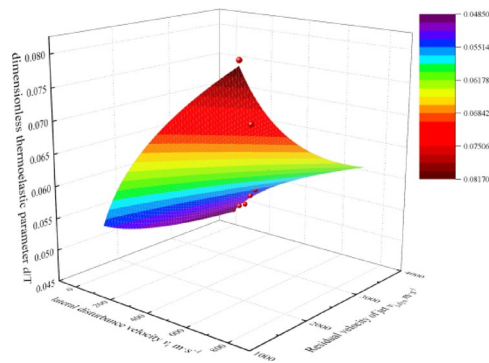


Fig. 12. Dimension prediction model of d/T .

$$\frac{d_{dyn}}{T} = 0.028 \left(\frac{v_t t_r}{T} \right)^{0.487} \left(\frac{v_{j,dyn} t_r}{T} \right)^{-0.745} + 0.0438 \tag{12}$$

From Fig. 12, it can be seen that the fitting degree R^2 value of the formula is 0.956, that is, the interpretation strength is 95.6%. The expression obtained by dimensional analysis is in good agreement with the numerical simulation results, and the consistency with the numerical simulation results is high. The dimensionless analysis model can better predict the diameter behind the jet target under dynamic conditions.

In the calculation of the residual parameters after the jet dynamic target, this paper follows the $v^2 d$ criterion proposed by HELD to consider it, and the combined formulas (10) and (12) are available.

$$v^2 d_{dyn} = \left(0.028 \left(\frac{v_t t_r}{T} \right)^{0.487} \left(\frac{v_{j,dyn} t_r}{T} \right)^{-0.745} + 0.0438 \right) \left[0.572 - 0.039 v_{j0} \left(3.423^{13.322 \frac{v_t}{v_{j0}}} \right)^{1.332} \right]^2 \tag{13}$$

Based on Eq. (12), the residual parameters behind the jet dynamic target with lateral disturbance velocity v_t in the range of 50–750 $\text{m}\cdot\text{s}^{-1}$ are compared with the predicted results of dimensional analysis, as shown in Fig. 13.

The dimensional analysis results are in good agreement with the numerical simulation results, and the consistency with the numerical simulation results is high. The dynamic penetration prediction model of the jet shows good consistency in the range of $v_t = 50 \text{ m}\cdot\text{s}^{-1}$ –750 $\text{m}\cdot\text{s}^{-1}$. The model can effectively describe the evolution process of the $v^2 d$ value of jet behind the plate under different dynamic conditions.

Validation of prediction model

In order to further analyze the effectiveness of the prediction model, We have built a dynamic penetration test system of shaped charge jet, and its schematic diagram is shown in Fig. 14. In the dynamic test, six groups of rocket motors were used to push the shaped charge. By placing the SCJ perpendicular to the thrust direction of the rockets, a transverse disturbance velocity is given to the SCJ and the target plates. When the probe rod contacts the siding, the trigger in the probe rod acts to transmit the signal to the fuse of SCJ to create shaped charge jet to penetrate the multilayer target plate with finite thickness below.

We calculate the lateral velocity of the SCJ propelled by the rocket through the equidistant marker line on the orbital base, as shown in Fig. 15, and combined with the results of high-speed photography. The test results of the

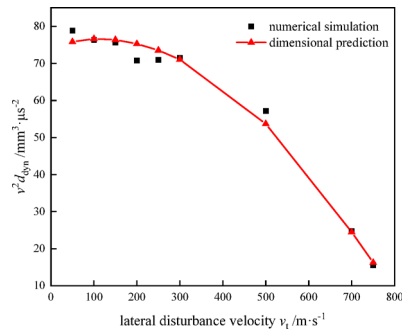


Fig. 13. Prediction curve of dynamic residual parameter v^2d .

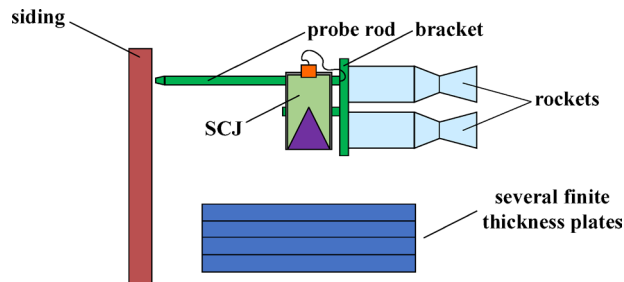


Fig. 14. Dynamic test system diagram.



Fig. 15. Photography record of SCJ dynamic test.

dynamic penetration depth of the shaped charge jet at different relative speeds were obtained. The flight speed is $274 \text{ m} \cdot \text{s}^{-1}$ by high-speed photography, and the test results are shown in Fig. 15.

The dimensional analysis model is compared with the dynamic test results, as shown in Fig. 16.

Comparing the experimental data with the prediction model results, it can be seen that the relative error of each result is below 14%, showing good consistency. It is verified that the regression model has certain accuracy in estimating the dynamic penetration power of jet at different speeds. The potential difference between the model prediction and the test results is mainly due to the fact that in the dynamic penetration power test, the warhead movement is affected by many factors such as the flatness of the track, the synchronization difference between the rocket engines, and the overload disturbance of the rocket pulley, which further increases the penetration depth runout range of the shaped charge warhead, so that there is a certain error between the model prediction and the experimental results.

Conclusion

We use the numerical simulation method to simulate the process of dynamic penetration of shaped charge jet into the charge behind the target. Based on the virtual origin and dimensional analysis, the engineering prediction model of jet residual velocity and jet diameter behind the target is established. The static and dynamic tests of shaped charge jet are carried out, and the validity of numerical simulation and prediction model is verified. The main conclusions are as follows:

1. When the lateral disturbance velocity is in the range of 50–750 m/s, the velocity behind the jet dynamic target shows an exponential decline trend. The diameter behind the jet target increases exponentially.
2. Based on the virtual origin theory and dimensional analysis method, considering the influence of transverse disturbance velocity, jet and target strength, it is found that there is a good exponential relationship between the dimensionless variables $v_{i,dyn}/v_{j0}$, d/T and their respective variables.
3. By comparing the numerical simulation, prediction model and experimental data under different lateral disturbance velocities, it is found that the relative errors between the established prediction model, numerical

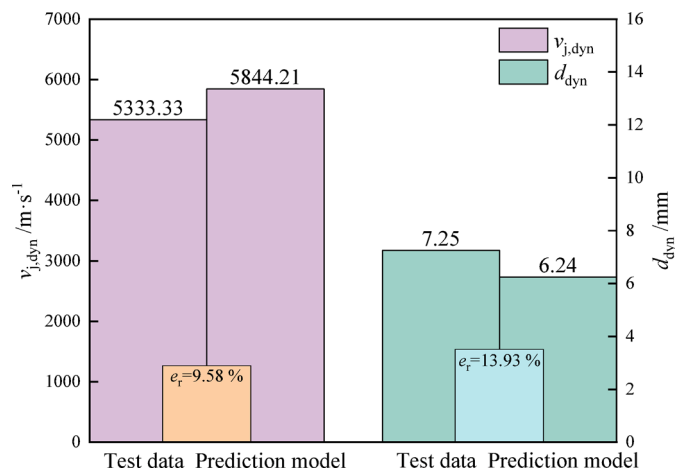


Fig. 16. Comparison of the experimental results with the prediction model.

simulation and experimental data are all below 14%, which has good consistency. The established engineering model can effectively estimate the parameter v^2d behind the jet target under dynamic conditions.

Data availability

Data sets generated during the current study are available from the corresponding author (Yizhen Wang) on reasonable request. Restrictions apply to the availability of these data, which were used under license for the current study, and so are not publicly available.

Received: 5 March 2025; Accepted: 21 October 2025

Published online: 24 November 2025

References

- Hao, Z., Wang, Z., Xu, Y., Duan, C. & Wang, Y. Study on the detonation wave propagation of shaped charge with three-layer liner and its driving characteristics to liner. *Sci. Rep.* **14**, 8778 (2024).
- Park, J. & Kwon, S. Study on the penetration performance of a double-angle linear shaped charge: Performance improvement and miniaturization. *Aerospace* **11**, 310 (2024).
- Guo, Y., Peng, S. & Yang, R. Experimental and numerical simulation study on penetration damage effect of parabolic-shaped charge. *J. Braz. Soc. Mech. Sci. Eng.* **47**, 91 (2025).
- Zhang, Z. et al. Energy output of shaped charge in underwater explosion. *Phys. Fluids* **36**(12), 126145 (2024).
- Fang, Y. Z. et al. Study on penetration law of shaped charge jet considering shape distribution characteristics. *Trans. Beijing Inst. Technol.* **43**(10), 1047–1058 (2023).
- Helte, A., Lundgren, J. & Candle, J. The interaction between a shaped charge jet and a single moving plate. *Def. Technol.* **31**, 1–13 (2024).
- Frankel, I. & Weihs, D. Hydrodynamic theory of glancing impact. *J. Fluid Mech.* **216**, 213–229 (1990).
- Cao, P. et al. Numerical simulation of rod jet penetration moving target. *J. Ordnance Equip. Eng.* **42**(04), 86–90 (2021).
- Luttwak G, Luttwak A. Moving plate perforation analytic model and numerical simulations. Proceedings of the 21st International Symposium on Ballistics, Adelaide, Australia: International Ballistics Committee, 976–983 (2004)
- Li, G. & Chen, X. W. A compressible model of radial crater growth by shaped-charge jet penetration. *Explos. Shock Waves* **42**(07), 97–105 (2022).
- Yadav, H. S. Interaction of a metallic jet with a moving target. *Propell. Explos. Pyrotech.* **13**(3), 74–79 (2010).
- Han, S. F. *Simulation research on sunder armor oblique penetrate high speed movement* (North University of China, 2015).
- Zhu, D. B. & Li, J. Y. Disturbance on an armor-piercing jet caused by an explosive armor. *Acta Armamentarii* **12**(001), 46–53 (1991).
- Tamer, E., Li, Q. M. & Ahmed, E. Experimental and numerical investigation of zirconium jet performance with different liner shapes design. *Def. Technol.* **18**(01), 12–16 (2022).
- Helte, A. & Lide, N. E. The role of kelvin-helmholtz instabilities on shaped charge jet interaction with reactive armor plates. *J. Appl. Mech.* **77**(5), 051805 (2010).
- Wu, Y. & Chen, C. Detonation wave propagation of double-layer shaped charge and its driving characteristics to the liner. *Shock Vib.* **2023**(1), 4201663 (2023).
- Ma, X. J., Kong, D. R. & Shi, Y. C. Experimental and numerical investigation of blast loads induced by moving charge explosion. *Structures* **47**, 2037–2049 (2023).
- Li, J. R. et al. Numerical study and theoretical model of shaped charge jet penetrating into thick-walled target with following velocity. *Int. J. Aerosp. Eng.* **17**, 7646255 (2024).
- Jia, X. et al. Theoretical model and numerical study of shaped charge jet penetrating into thick moving target. *Acta Armamentarii* **40**(08), 1553–1561 (2019).

Acknowledgements

This work was supported by the Shanxi province basic research program free exploration youth fund project (Grant Nos. 202203021212136).

Author contributions

Xuepeng Zhang: Conceptualization, methodology, software, validation, investigation, data curation, formal analysis, writing—original draft preparation, project administration. Can Xu: Conceptualization, formal analysis, investigation, data curation, writing—review and editing, supervision. Yizhen Wang: formal analysis, investigation, supervision. Jianping Yin: formal analysis, investigation, supervision. Jianya Yi: formal analysis, investigation, supervision. Xudong Li: formal analysis, investigation, supervision. All authors have read and agreed to the published version of the manuscript.

Declarations

Competing interests

The authors declare no competing interests.

Additional information

Correspondence and requests for materials should be addressed to J.Y.

Reprints and permissions information is available at www.nature.com/reprints.

Publisher's note Springer Nature remains neutral with regard to jurisdictional claims in published maps and institutional affiliations.

Open Access This article is licensed under a Creative Commons Attribution-NonCommercial-NoDerivatives 4.0 International License, which permits any non-commercial use, sharing, distribution and reproduction in any medium or format, as long as you give appropriate credit to the original author(s) and the source, provide a link to the Creative Commons licence, and indicate if you modified the licensed material. You do not have permission under this licence to share adapted material derived from this article or parts of it. The images or other third party material in this article are included in the article's Creative Commons licence, unless indicated otherwise in a credit line to the material. If material is not included in the article's Creative Commons licence and your intended use is not permitted by statutory regulation or exceeds the permitted use, you will need to obtain permission directly from the copyright holder. To view a copy of this licence, visit <http://creativecommons.org/licenses/by-nc-nd/4.0/>.

© The Author(s) 2025